

## EVALUATION AND ASSESSMENT OF THE ASPIRE CONCEPT: A NEW INTEGRATED MC-SI CELL AND MODULE DESIGN FOR HIGH EFFICIENCIES

I.G. Romijn, A.A. Mewe, E. Kossen, I. Cesar, E.E. Bende, M. N. van den Donker<sup>2</sup>, P. van Eijk<sup>3</sup>, E. Granneman<sup>4</sup>, P. Vermont<sup>4</sup>,  
A.W. Weeber

<sup>1</sup>ECN Solar Energy, P.O. Box 1, 1755 ZG Petten, The Netherlands  
Phone: +31 224 564309; Fax: +31 224 568214; email: [romijn@ecn.nl](mailto:romijn@ecn.nl)

<sup>2</sup>Solland Solar, Bohr 10, 6422 RL Heerlen, The Netherlands

<sup>3</sup>Ferro Electronic Material Systems, Frontstraat 2, 5405 PB Uden, The Netherlands

<sup>4</sup>Levitech BV, Versterkerstraat 10, 1322 AP Almere, The Netherlands

### ABSTRACT:

The majority of commercial crystalline Si cell production is carried out on p-type crystalline silicon using an H-patterned cell concept with full aluminum rear surface. To decrease the Euro/Watt-peak price, higher efficiencies have to be reached while using less material. In this paper, the ASPIRe cell concept is put forward as a candidate to further these goals. In the ASPIRe cell two technologies are combined: 1) Metal wrap through technology; reducing the front metal coverage and moving all contacts to the rear, and 2) dielectric rear side passivation; reducing the bow for thinner wafers, increasing the rear passivation and reflection, and reducing the metal consumption due to rear grid instead of full area aluminum. To evaluate the ASPIRe concept, ASPIRe cells have been modeled using 2D simulation methods. Depending on the resistivity of the rear side metallization, and on the full area BSF quality, a relative efficiency gain of 2 to 4% was calculated for ASPIRe cells compared to full aluminum rear MWT cells. Using industrially applied Al<sub>2</sub>O<sub>3</sub> as rear passivating layer and optimized rear metallization patterns, ASPIRe cells with higher  $J_{sc} \cdot V_{oc}$  and FFs close to their full Al references were made. One final bottleneck for the industrialization of the ASPIRe concept is a cost effective way to form of a good local BSF below the metal lines. Cost and environmental calculations show that, once this is solved, the ASPIRe concept indeed enables lower Euro/Watt-peak and shorter energy-payback-times than the standard cell concept.

Keywords: multi crystalline, metal-wrap-through, back contact, bifacial, aluminum-oxide

### 1 INTRODUCTION

The use of standard cell technology with a full aluminum rear surface and interconnection tabs on both front and rear side on thinner wafers will cause a drop in cell efficiency due to a non optimal rear surface, while breakage will occur due warping which is caused by different thermal expansion coefficients of the silicon and the aluminum-silicon alloy. Furthermore, stresses induced in the cells by the tabbing-stringing from the front to the rear surface of the cells will cause even more breakage. The logical step to overcome these drawbacks is to develop a fully back-contacted cell concept without a full aluminum rear surface. Using a dielectric layer with open rear metallization will reduce the bowing of thinner solar cells and increase the rear surface passivation and rear reflection of the encapsulated solar cells when compared to a full aluminum rear surface. Furthermore, the reduced Al consumption will result in lower costs.

One of the new concepts that is currently investigated at ECN is the ASPIRe (All Sides Passivated and Integrated at the Rear) cell, which combines our Metal Wrap Through (MWT) and rear surface passivation (PASHA) technologies [1, 2]. With our MWT cell (full area Al BSF) and module technology we have reached 17.9% cell, and 17.0% module efficiency (aperture area) on multi crystalline wafer material, published as a new World Record in December 2009 [3]. ASPIRe has the potential to increase this efficiency by an improved rear-side passivation and an enhanced reflection.

At ECN we aim to reach high efficiencies using technologies that integrate the cell and module processing and can be easily industrialized. The back contacted MWT cell technologies can be seen as a first step towards development of even more advanced cell structures like Emitter Wrap Through (EWT) and Interdigitated-Back-Contact (IBC) solar cells and modules, allowing even higher efficiencies. In these cell

concepts, the metallization is completely removed from the front surface while at the same time passivation of the rear surface becomes even more important. Industrialization of concepts such as EWT and IBC will benefit a lot from a deeper understanding of the underlying mechanisms and bottlenecks of, and development of simulation methods for, the ASPIRe cells. This will be crucial for further research towards these cell concepts.

### 2 ASPIRE CELLS

#### 2.1 From standard cell concept to ASPIRe

As proof of principle for the ASPIRe cell concept we started with a straight forward concept, deviating as little as possible from standard mc-Si cell processing with a H-patterned front and a full aluminum rear side. Two adjustments to this standard cell concept are combined in the new ASPIRe cell concept. On the one hand, an MWT structure is applied: Using a metal wrap through design with 16 holes in the wafer, the front metallization coverage can be reduced by over 2% [4]. On the other hand, our PASHA (Passivated All Sides H-pattern) concept is applied. In this concept the rear surface is passivated by a dielectric coating reducing the rear metallization coverage [2]. These two separate steps are combined in the ASPIRe concept. Cross sections of all concepts are shown in figure 1. In figure 2, the various process flows are shown.

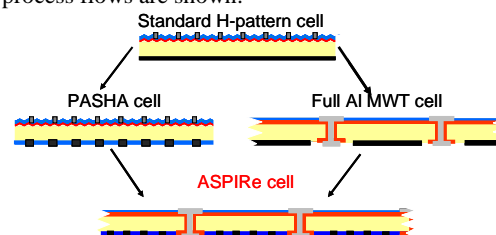
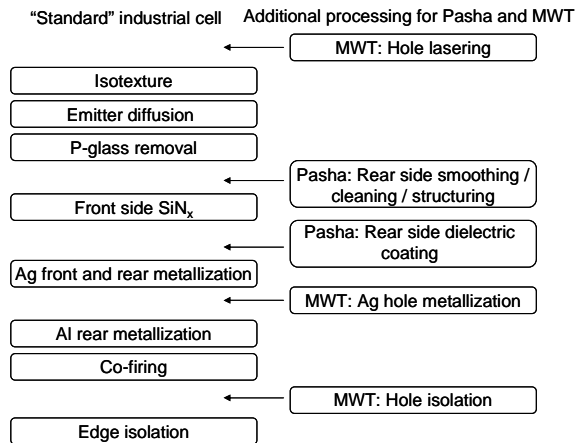


Figure1: Evolution ASPIRe from standard cell concept.



**Figure 2:** Process flows for the different cell concepts. On the left, the process flow for standard, H-patterned p-type solar cells is shown. On the right, additional processing steps for the MWT and PASHA concepts are indicated. For the ASPIRe cell concept, all additional process steps need to be done.

The advantage of the ASPIRe cell over the bifacial H-pattern PASHA solar cell is - besides the lower front metal coverage - the modular rear contact design. This offers more freedom in optimizing the rear metallization pattern in order to obtain higher FF, especially in the module. Both PASHA and ASPIRe cells are truly bifacial, no additional metal layer is used on the rear surface.

For the first ASPIRe cells single Silicon Nitride ( $\text{SiN}_x$ ) layers were used to passivate both the front and rear surface. Contacts were made using simultaneous “firing through” of Ag for the front and Al for the rear surface.

The first ASPIRe cells had a relatively large  $\text{SiN}_x$  surface coverage ( $\sim 90$ ), therefore a low contact area and a non-optimized pattern on the rear side. To get good fill factors, the rear metallization had to be electrically short circuited. For these cells, we were able to obtain a gain in  $J_{sc} \cdot V_{oc}$  of 0.5% absolute compared to a full Al reference cell. The FF however, was still lower, which resulted in a 0.4% absolute lower efficiency for ASPIRe compared to the full Al MWT reference group [1].

The optimal cell efficiency will be determined by a trade-off between rear surface passivation (by the dielectric layer and the local BSF, visible in  $J_{sc} \cdot V_{oc}$ ) on the one hand and fill-factor (determined by contact and line resistance, pattern and metallization fraction) on the other hand. In the next sections of this paper we show that additional problems are encountered when using higher metallization fractions and how they can be tackled.

## 2.2 Simulations on ASPIRe cells

To gain more insight into the ASPIRe concept and the potential efficiency gain, simulations were performed for both  $J_{sc} \cdot V_{oc}$  gain and FF loss with decreasing metal fraction. The computations for  $J_{sc}$  and  $V_{oc}$  were done with the 2D program Microtec [5], while the computations for the FF were done with the 2D program Abaqus. This means that  $J_{sc} \cdot V_{oc}$  gain simulations can be executed regardless of the chosen concept (Pasha or ASPIRe) and metallization pattern. In this way, possible improvements in the Al BSF quality and dielectric passivation can be easily implemented in the model. The FF has been

calculated for both ASPIRe and PASHA cells. Combining the two simulations, predictions on efficiency gain can be done.

In figure 3, the relative gain for  $J_{sc} \cdot V_{oc}$  and losses for FF are shown relative to a full area Al BSF. Assumptions for this computation are a bulk lifetime ( $\tau_{bulk}$ )  $\sim 20 \mu\text{s}$  for standard multi crystalline Si; rear reflection ( $R_{rear}$ ) of 95% for  $\text{SiN}_x$ , and 79% for aluminum; rear surface recombination velocity ( $S_{rear}$ ) of 25 cm/s for  $\text{SiN}_x$  and a local BSF with 7  $\mu\text{m}$  thickness, denoted as “good” (typically giving an  $S_{eff}$  of 200 cm/s) or a local BSF with 2  $\mu\text{m}$  thickness, denoted as “medium” (typically giving an  $S_{eff}$  of 1000 cm/s). The total rear surface recombination and reflections will be determined by weighted averages of the local BSF and the  $\text{SiN}_x$ . In two cases (blue and green line in figure 3), the BSF quality for the local BSF is assumed to be the same as for the full area Al reference cell. As can be seen from the figure, the worse the full-area BSF quality, the higher the gain if the rear aluminum is replaced by a better passivating layer. In reality, the local BSF quality when the aluminum is fired through a dielectric layer, will not be as good as the full-area (non-fired through) aluminum BSF quality. In that case, the  $J_{sc} \cdot V_{oc}$  gain will be less for ASPIRe/Pasha (red line).

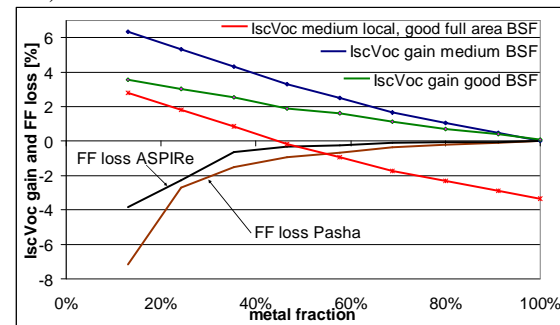


**Figure 3:** Simulated gain in  $J_{sc} \cdot V_{oc}$  and losses in FF for ASPIRe and Pasha cells

The main contribution to gain in  $J_{sc} \cdot V_{oc}$  comes from the enhanced rear reflection, while the surface passivation contributes around 1-2% relative at 10% metallization fractions. The FF for Pasha and ASPIRe is for a large part determined by the line resistance of the aluminum lines at the rear, for another part by the base resistivity of the p-type Si material. The FF loss for low metal fractions is more pronounced in Pasha than in ASPIRe cells, as the modular design of ASPIRe gives more options to optimize the pattern and for instance reduce the aluminum line length.

In figure 4, both contributions are added to show the possible efficiency gain for ASPIRe cells compared to a full aluminum MWT reference cell. This gain lies between 0.2% (good full area BSF, medium local BSF) and 3.7% (full area and local BSF both of medium quality)

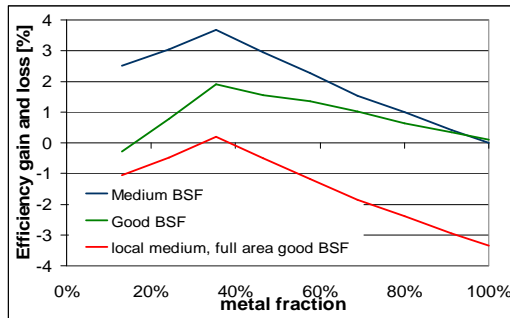


**Figure 4:** Relative gain in efficiency for ASPIRe cells compared to a full aluminum reference MWT cell

### 2.3 Optimization of ASPIRe design – rear metallization fraction

For ASPIRe cells, the rear side metallization structure has been optimized using a home made software program based on analytical calculation of the lowest series resistance for a certain metallization fraction. The most important input parameters used for the calculation are contact and line resistance of the aluminum paste, minimal aluminum line width, wafer thickness and wafer resistivity. Newly designed patterns for different metal fractions are shown in figure 5. The metallization converges towards one base contact point. On the rear of the ASPIRe cells are in total 5x5 base contact points, which means the patterns from figure 5 are repeated 25 times.

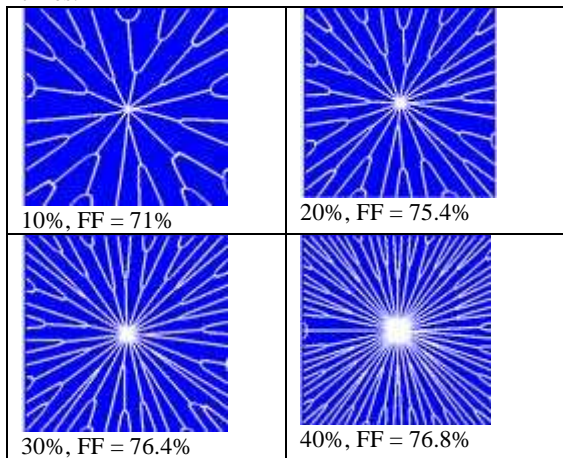


**Figure 5:** Rear metallization patterns of one unit cell for ASPIRe with calculated FFs.

Besides optimizing the metal on the cells, also the resistive losses from cell to module were investigated. For the ASPIRe cells, the same interconnection technology as for the ECN-full aluminum-MWT concept can be used. Both base and emitter contacts are located at the rear side of the cell. The cells are picked and placed onto an interconnecting foil, where the contacts are glued [3,4]. For the ASPIRe simulations, the number of base contact points has been varied and experimentally evaluated. The final choice was for 5x5 base contact points [1].

### 3 ASPIRE CELL RESULTS

ASPIRe cells were made on 243 cm<sup>2</sup> p-type mc-Si using the different optimized rear side screens, with a rear metal fraction ranging from 7 to 40%. Two different wafer thicknesses, 135 and 160 μm, were used. For the rear side passivation, single SiN<sub>x</sub> layers were used.

Contacts were made using co-firing through. In the following sections, the IV and FF results will be analyzed in more detail.

#### 3.1 FF results:

The average values for FF of ASPIRe cells with different metal fractions and two different wafer thicknesses are shown in figure 6.

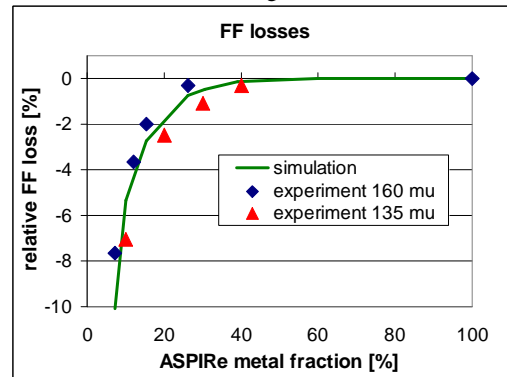


**Figure 6:** FF for ASPIRe cells with different metal fractions and two different wafer thicknesses. Simulation was done on cells with a thickness of 160 μm.

With new ASPIRe rear metallization patterns, FFs of over 76.5% have been reached on 160 μm ASPIRe cells for metal fractions of 26% or higher, only 0.3% relative lower than the 77.2% reached with a full area Al rear side. These values correspond quite nicely to those calculated with the simulations as can be seen in figure 6. For the thinner cells (135 μm), the FFs achieved on ASPIRe cells are a little lower. This is due to the increased wafer resistivity of the base material at the same doping levels. However, also for these cells the FF approach those of the full Al reference cell for metal fractions above 40%.

#### 3.2 J<sub>sc</sub>\*V<sub>oc</sub> results: rear side passivation

The values for J<sub>sc</sub> and V<sub>oc</sub> of the ASPIRe cells are shown in figures 7 and 8.

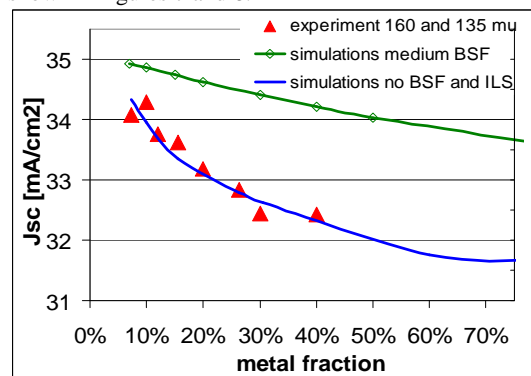


**Figure 7:** J<sub>sc</sub> measurements and simulations for ASPIRe

In the same graphs, the results of two simulations are shown. For the first simulation (shown as green line), a ‘medium’ local BSF was assumed below the metal lines, and no additional losses due to for instance inversion layer shunting (ILS, also referred to as “parasitic shunting”) were incorporated. Clearly, the experimentally found values for J<sub>sc</sub> and V<sub>oc</sub> of the ASPIRe cells are lower than those calculated with the medium BSF model,

especially at higher metallization fractions. At 0% metallization, the simulated curve converges with the ASPIRe cell results, indicating that the value of  $S_{SiN_x}$  and  $R_{SiN_x}$  are adequate.

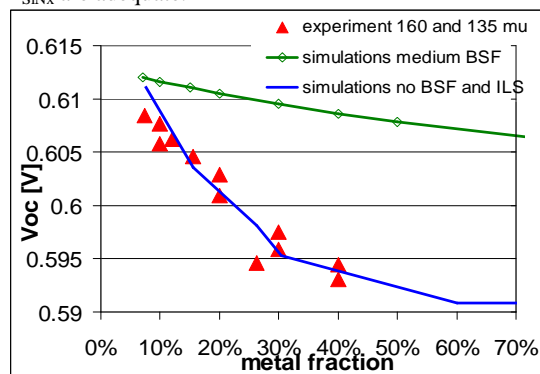


**Figure 8:**  $V_{oc}$  measurements and simulations for ASPIRe

The steeper downwards slope for the ASPIRe cells can be attributed to two factors:

1) Inversion-layer shunts [6-9]. Fixed positive charges at the passivating  $SiN_x$ -Si interface will create a negatively charged inversion layer. At the aluminum contacts, at the interface between the  $SiN_x$  and Al, this will cause a leakage current called inversion-layer shunt. As the metallization fraction increases there are more and more  $SiN_x$ -Al interfaces on the rear surface (see figure 5). Therefore the contribution of inversion-layer shunt will increase for higher metal fractions, causing a severe drop in both  $J_{sc}$  and  $V_{oc}$ .

2) The local BSF, formed by firing the aluminum through the  $SiN_x$ , is not even of medium quality resulting in a higher  $S_{Al}$  than the  $1000 \text{ cm/s}$  assumed. As the metallization fraction increases, this effect becomes more and more pronounced decreasing  $V_{oc}$  and  $J_{sc}$ .

The second simulation curve (blue) takes both effects into account. In this case, no BSF is assumed below the metal contacts (giving a  $S_{eff, rear} > 10000 \text{ cm/s}$ ) and the effect of inversion layer shunting is included. As can be seen in graphs 7 and 8, including both effects can explain the rapid decrease in  $J_{sc}$  and  $V_{oc}$  for higher metal fractions. In order to improve the ASPIRe cells, both problems will have to be solved.

### 3.3 $Al_2O_3$ passivating layer

An effective solution to the problem of inversion layer shunting on p-type surfaces that has been reported by many parties recently is the use of  $Al_2O_3$  layers as passivating layer [10,11]. Surface passivation by  $Al_2O_3$  layers can reduce the effective recombination velocity below  $10 \text{ cm/s}$  on test structures, both by a very good chemical passivation and a field effect brought upon by a very high negative surface density ( $-10^{12} - -10^{13} \text{ cm}^{-2}$ ) [12-14]. Opposite to the  $SiN_x$  case, the negative surface charges will result in a positively charged inversion layer. On p-type surfaces this will enhance the passivation instead of cause shunting at the contacts.

We tested **single, non-capped** thin  $Al_2O_3$  layers as rear side passivating layers on both H-patterned PASHA and MWT ASPIRe cells. The  $Al_2O_3$  layers were deposited by Levitech B.V. using the Levitrack, a newly developed tool. With this tool, layers are deposited using an in-line, continuous ALD process [15,16]. In his paper [15] Cesar et al. already presented Pasha cells made with  $Al_2O_3$  rear surface

passivation. However, in that case the  $Al_2O_3$  layers were deposited with a laboratory ALD reactor and metal contacts were formed by locally opening the rear dielectric layer. For our cells, we applied the most simple process: the metal contacts were again formed by co-firing through the front and rear dielectric layer.

The IV results of the cells, including their full aluminum references are shown in table 1. All cells, including an extra ASPIRe group with  $SiN_x$  passivation were processed on  $243 \text{ cm}^2$  p-type mc-Si neighboring wafers of  $160 \mu\text{m}$ . For both PASHA and ASPIRe a rear side metal fraction of 15% was used.

cell	$J_{sc}$ [mA/cm <sup>2</sup> ]	$V_{oc}$ [mV]	$J_{sc} \cdot V_{oc}$	FF [%]	$\eta$ [%]
MWT ref	35.4	618	21.9	77.3	16.9
ASPIRe $Al_2O_3$	35.9	613	22.0	74.9	16.5
ASPIRe $SiN_x$	34.2	602	20.5	75.3	15.5
H-ref	35.0	617	21.6	77.3	16.7
Pasha $Al_2O_3$	35.4	610	21.6	72.6	15.7

**Table 1:** Average IV results, using 15 wafers per group

As expected, the  $J_{sc}$  and  $V_{oc}$  for  $Al_2O_3$  ASPIRes improve considerably with respect to the  $SiN_x$  ASPIRe cells. Moreover, the  $J_{sc} \cdot V_{oc}$  value for the  $Al_2O_3$  ASPIRe now exceeds that of the full aluminum reference. Furthermore, the large advantage of MWT cells over H-patterned cells becomes clear: Not only the FF for ASPIRe is improved by more than 2% absolute with respect to the PASHA cells for the same rear metal percentage, also the  $J_{sc}$  is improved by  $0.5 \text{ mA/cm}^2$  due to the lower front metal coverage. A highest efficiency for ASPIRe of 16.6% has been obtained.

Even though the  $J_{sc}$  improved a lot by using rear  $Al_2O_3$  layers, the  $V_{oc}$  values still remained behind compared to the full aluminum references and the calculated efficiency gain has not been obtained. This can be explained by the insufficiently formed local BSFs for the Pasha and ASPIRe cells [15]. Using firing through of aluminum contacts while keeping the dielectric layer passivation intact, a local BSF thickness of only 1-2  $\mu\text{m}$  could be formed.

Two examples of a BSF formed on bare Si and a BSF formed by firing through a  $SiN_x$  layer are shown in figure 9. The BSF shown in figure 9b, formed by firing through, is much thinner than that formed on a bare Si wafer (fig 9a).

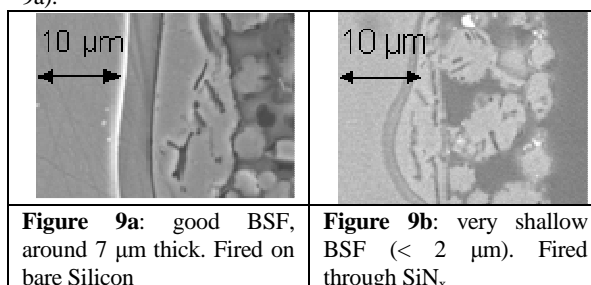


**Figure 9a:** good BSF, around  $7 \mu\text{m}$  thick. Fired on bare Silicon

**Figure 9b:** very shallow BSF ( $< 2 \mu\text{m}$ ). Fired through  $SiN_x$

In figure 10 internal quantum efficiency (IQE) graphs are shown for the different MWT cells from table 1 including fits made with PC1D. The values fitted with PC1D are shown in table 2. The PC1D parameters governing the blue response of the cell ( $S_{front}$ ,  $R_{front}$ , emitter sheet resistivity) and those regarding wafer quality (bulk lifetime, bulk doping level) were kept the same for all cells.

Only the parameters governing the red response of the cell ( $S_{\text{rear}}$ ,  $R_{\text{rear}}$ ) were found to be deviating for the differently passivated cells.

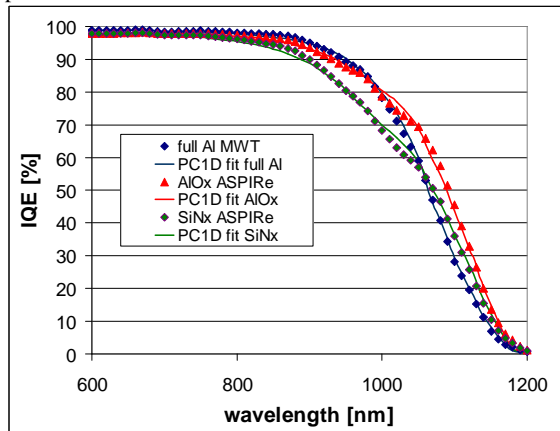


**Figure 10:** IQE results for the different MWT cells including PC1D fits. The IQE curves are overlapping at lower wavelengths, but start to deviate at wavelengths above 800 nm indicating differences in  $S_{\text{rear}}$  and  $R_{\text{rear}}$

	Full Al MWT	Al <sub>2</sub> O <sub>3</sub> ASPIRe	SiN <sub>x</sub> ASPIRe
Emitter (W/sq)	66	66	66
Tau_bulk (μs)	50	50	50
S <sub>rear</sub> (cm/s)	200	450	1500
R <sub>rear</sub> (%)	70	85	84

**Table 2:** values fitted with PC1D from IQE curves for the different MWT cells

The IQE values at 1000 nm are around 80% for both the full Al MWT and the Al<sub>2</sub>O<sub>3</sub> ASPIRe, while the value for the SiN<sub>x</sub> ASPIRe is clearly lower, around 69%. This indicates that the Al<sub>2</sub>O<sub>3</sub> passivation works very well. Nevertheless, the full Al MWT cell was fitted with the lowest  $S_{\text{rear}}$  indicating the best rear surface passivation, while the  $S_{\text{rear}}$  for the Al<sub>2</sub>O<sub>3</sub> ASPIRe was a bit higher. This stems from the slightly lower response at 900 nm. For both ASPIRe cells, the rear reflection is much better than that of the full Al cell. The observed gain in  $J_{\text{sc}}$  for the Al<sub>2</sub>O<sub>3</sub> ASPIRe stems solely from the increased rear reflection while the loss in  $V_{\text{oc}}$  can be explained by the higher  $S_{\text{rear}}$ .

A good BSF, with a thickness of 7-10 μm will have a  $S_{\text{rear}}$  of ~ 200 cm/s. This is the case for the full area Al MWT reference. For the ASPIRe cells however, this value is not obtained. Even with the Al<sub>2</sub>O<sub>3</sub> passivating layer, which does not cause inversion layer shunting, a lowest value for  $S_{\text{rear}}$  of 450 cm/s is reached. In a first order approximation, the total  $S_{\text{rear}}$  can be seen as a weighted average of the recombination velocities of the local BSF and the rear passivating layer. Assuming that 85% of the rear surface is passivated adequately by Al<sub>2</sub>O<sub>3</sub> with a maximum  $S_{\text{rear}}$  of 25 cm/s, this means that the remaining 15% passivated by the local BSF has a  $S_{\text{rear}}$  of at least 3000 cm/s. To obtain a total  $S_{\text{rear}}$  below 200 cm/s, the local BSF should at least be of medium quality with an  $S_{\text{rear}}$  in the order of 1000 cm/s, which means that the BSF should be at least 2 μm thick (see figure 9a and 9b).

Thicker BSFs than 2 μm can be made using firing through the dielectric layer, however up to now at the costs of the passivation by the dielectric layer. Firing at too extreme conditions will destroy its passivating qualities.

This process still needs to be improved and optimized. Another option is to form the local BSF in a separate process step by for instance local boron diffusion or laser firing of the metal contacts [17].

#### 4 BOTTLENECKS FOR INDUSTRIALISATION OF ASPIRe

The first ASPIRe cells suffered from several issues which prevented industrialization: low FF due to non optimized rear metallization, low  $J_{\text{sc}}$  and  $V_{\text{oc}}$  due to inversion layer shunting of the SiN<sub>x</sub> layer and a bad local BSF formation.

In this paper we showed that using an improved rear side metallization design, FF very close to those of the full Al reference can be obtained for a 30% metal fraction. Furthermore, using industrial Al<sub>2</sub>O<sub>3</sub> layers, the problem of inversion layer shunting can be solved. This means that only 1 bottleneck remains for the industrialization of ASPIRe cells: the formation of a medium to good local BSF below the metal contacts

One of the conditions for industrialization of a new concept is a simple process flow, that does not deviate strongly from the standard process flow nor adds many additional steps. This is why contacting using co-firing through the front and rear passivating coating was chosen for the PASHA and ASPIRe cells. Once the issue of the local BSF formation has been solved, the ASPIRe cell can be implemented into industrial solar cell lines. Contacting into a module will be done in the same way as for the ECN-MWT cells, which has been extensively tested and proven in the last few years [18].

#### 5 ASSESSMENT OF ASPIRe AS FUTURE CELL CONCEPT AND COMPARISON TO OTHER CONCEPTS

A new cell concept will be attractive for industrialization if the efficiencies are high at low costs, in other words: the costs/Wp should be lower compared to the standard cell concept. When the local BSF formation is adequate, efficiency gains of 2-4% relative to a full aluminum MWT cell could be obtained with ASPIRe. The gain achieved will then depend on the BSF quality that is obtained for the full aluminum reference cell. If the formation of a good local BSF can be achieved using co-firing through, the complexity of the process hardly increases. In fact, the overall processing costs of ASPIRe will decrease due to less Ag (MWT pattern on front; no more busbars) and Al (only 30% at most on rear) usage. It is expected that the single thin dielectric Al<sub>2</sub>O<sub>3</sub> layer reduces the costs of ownership significantly as compared to for instance PERC cells where thick (100nm) stacked layers are used [11].

Compared to other cell concepts using rear surface passivation such as LFC [17] or PERC cells [11,19] the ASPIRe cell does not have the highest gain potential. Especially the FF benefits from the additional metal layer that these other concepts use on top of their rear passivating layer. However, the advantages of the ASPIRe concept over for instance PERC and LFC are:

- The rear dielectric layer does not have to be covered by an aluminum (or other) paste that could harm its passivation quality during firing, or long-term stability of the passivation. This means a single, thin

passivating layer like Al<sub>2</sub>O<sub>3</sub> can be used and no stacks are needed;

- Less aluminum usage reducing the Euro/Watt-peak;
- The rear reflector below the cell can be tuned independently from the metallization enabling higher reflections in the module

Besides cost/Watt-peak, also the environmental impact of processing a certain concept needs to be considered. In order to calculate these impacts, ASPIRe modules ( $\eta=16.3\%$ ) were compared to standard H-pattern modules ( $\eta=14\%$ ) and a standard full Al MWT module ( $\eta=15.9\%$ ). The energy payback times (EPBT) are calculated based on the efficiencies above and the process flows shown in figure 2. For full area Al MWT and ASPIRe the EPBTs are equal, around 1 year. The EPBT for standard H-pattern modules is higher, around 1.7 year. Likewise, the carbon footprint is around 20 g CO<sub>2</sub> eq/kWh for the MWT modules, and 30 g CO<sub>2</sub> eq/kWh for the H-patterned modules.

## 6 CONCLUSIONS

In this paper the ASPIRe cell concept has been evaluated using both experiment and simulation. Thus far, ASPIRe cells suffered from several issues that prevented industrialization: Low FF due to non optimized rear metallization, low  $J_{sc}$  and  $V_{oc}$  due to inversion layer shunting of the SiN<sub>x</sub> layer and a bad local BSF formation. We show that using an improved rear side metallization design, FF very close to those of the full area Al reference can be obtained. Furthermore, we show that using industrial Al<sub>2</sub>O<sub>3</sub> layers, the problem of inversion layer shunting can be solved. This means that only 1 bottleneck remains for the industrialization of ASPIRe cells: the formation of a medium to good local BSF below the metal contacts. Once this issue is solved, relative efficiency gains between 2 and 4% are estimated. Using our high efficiency MWT processing [3], efficiencies of 17.9% have been reached on p-type mc-Si wafers. Combining the optimized ASPIRe cell concept with the high efficiency MWT processing, efficiencies of over 18.2% are well within reach. Industrializing the optimized ASPIRe concept will decrease the Euro/Watt-peak price, Energy Pay-back Time and Carbon footprint with respect to the full aluminum H-patterned cell concept making it a good candidate for future cell processing.

## 7 ACKNOWLEDGEMENTS

This work was financially supported by the Dutch Agentschap NL projects StarFire (EOS-ES program project IS063024) and Newton (EOS-KTO program project T09000212).

## 8 REFERENCES

- [1] A. A. Mewe et al., Proceedings 23<sup>rd</sup> EPVSEC, Valencia, September 2008
- [2] I. G. Romijn et al., Proceedings 33<sup>rd</sup> IEEE PV Specialist Conference, San Diego, 2008
- [3] M. Lamers et al., Proceedings 19<sup>th</sup> PVSEC, Jeju Korea, November 2009; This conference
- [4] A. W. Weeber et al; Proceedings of the 21<sup>st</sup> European PV SEC, Dresden, 2006; 605.
- [5] E. E. Bende, Proceedings 33<sup>rd</sup> IEEE PV Specialist

Conference, San Diego, May 2008

- [6] I. Cesar et al., Proceedings 24<sup>th</sup> EPVSEC, Hamburg, September 2009
- [7] S. Dauwe, Ph. D. Thesis, ISFH, 2004
- [8] S. Dauwe, L. Mittelstadt, A. Metz, R. Hezel, Prog. Photovoltaics Res. and Appl. **10**, 4, 2002, p271-278
- [9] Thesis Meemongkolkiat (check with Kay)
- [10] J. Benick, A. Richter, M. Hermle, S. Glunz, Phys. Stat Solidi RRL, **3**, 233, 2002
- [11] J. Schmidt, et al., Progress in Photovoltaics: Res. and Appl, **16**, 6, p461-466, 2008
- [12] B. Hoex et al., J. Appl Phys., **104**, 4, 2008 (044903/1)
- [13] G. Dingemans, M. van der Sanden, W. Kessels, Electrochemical and Solid-state letters, **13**, 3, 2009, p H76-79H
- [14] J. Schmidt et al., Proceedings 35<sup>th</sup> IEEE, Hawaii, 2010
- [15] I. Cesar et al., Proceedings 35<sup>th</sup> IEEE, Hawaii, 2010
- [16] E. Granneman et al., this conference
- [17] E. Schneiderlöchner, R. Preu, R. Lüdemann, S. Glunz, Progr. Photovolt. **10** (2002) p29
- [18] W. Eerenstein et al., this conference
- [19] P. Choulat et al., Proceedings 22<sup>nd</sup> EPVSEC, Milan, September 2009